A B3LYP Study on Repair of Guanyl and 8-Oxoguanyl Radical by Simultaneous Proton- and Electron-Transfer Reaction

Mami Yamamura, Tomoya Ichino, and Yasunori Yoshioka*

Chemistry Department for Materials, Graduate School of Engineering, Mie University, 1577 Kurima-machiya, Tsu, Mie 514-8507

Received July 28, 2010; E-mail: yyoshi@chem.mie-u.ac.jp

The proton transfers in base pairs of guanine (G)/8-oxoguanine (8G), $8G^{+\bullet}$–C, PhOH–G(-H)$^\bullet$, PhOH–8G(-H)$^\bullet$, and 8G–G(-H)$^\bullet$, have been theoretically examined in the gas phase at the B3LYP level of theory. For the $8G^{+\bullet}$–C base pair, the single proton transfer proceeds from N1($8G^{+\bullet}$) to N3(C) with the activation energy of 2.2 kcal mol^{-1}. The repairs of G(-H)$^\bullet$ and 8G(-H)$^\bullet$ bases to G and 8G have been studied by reaction with phenol, and the repair of G(-H)$^\bullet$ base has been also studied for the pair with the 8G base. These three reactions proceed under the PCET mechanism, in which the proton transfers through the σ-path, while the electron transfers through the π-path. For reactions with PhO$^\bullet$ and G(-H)$^\bullet$, 8G easily delivers a proton and electron to yield PhOH and G. It is expected that 8G functions to protect other bases and amino acids from oxidation.

DNA damage caused by one-electron oxidation of nucleobases leads to mutagenesis and carcinogenesis induced by ionizing radiation, high-intensity laser irradiation, and so on. Since guanine (G) base has the lowest ionization potential among DNA nucleobases,[1–4] the hole created in DNA duplex by one-electron oxidation ultimately migrates to end up at G through the DNA π stack.[5–12] Guanine radical cation ($G^{\bullet+}$) is the initial product of DNA one-electron oxidation to yield the $G^{\bullet+}$–C base pair with cytosine (C) base.[13–17]

It was found that the one-electron-oxidized $G^{\bullet+}$ induces quite rapid deprotonation with a rate constant of 10^7 s^{-1},[18] yielding a guanyl radical (G(-H)$^\bullet$) which is another precursor in DNA damage. It was shown theoretically that the hydrogen at N1 (Figure 1) site of G transfers as a proton toward the N3 site of cytosine, giving a base pair of guanyl radical and protonated cytosine (G(-H)$^\bullet$–C(+H$^+$)$^+$).[19–28] The activation energy was estimated to be 4.70 kcal mol^{-1} at the B3LYP/6-31++G**//B3LYP/6-31+G* level of theory,[23] being smaller than 14.8 kcal mol^{-1} of the double proton transfer in the G–C base pair.[29] The endothermic energy was estimated to be 1.32 kcal mol^{-1}, being also smaller than 9.8 kcal mol^{-1} in the G–C base pair.[23,29] The reactive G(-H)$^\bullet$ may be irreversibly degraded by reactive oxygen species and free radicals.

Oxidative damage of G and the reactions of $G^{\bullet+}$ with H_2O lead to formation an 8-oxoguanine (8G), which is also a species that can lead to mutagenesis and carcinogenesis. The 8G has been most extensively studied among chemical species in DNA oxidative damage.[30–36] The DNA polymerase misreads 8G as thymine, giving a base pair of 8G and adenine (8G–A) in place of cytosine of 8G–C. The 8G is also irreversibly degraded by reactive oxygen species and free radicals.

It was confirmed that 8G has lower ionization potential than G.[37] This shows the possibility that the 8G will be a hole sink of the DNA one-electron oxidation. The 8-oxoguanyl radical cation ($8G^{\bullet+}$) is expected to be formed as the $8G^{\bullet+}$–C base pair.

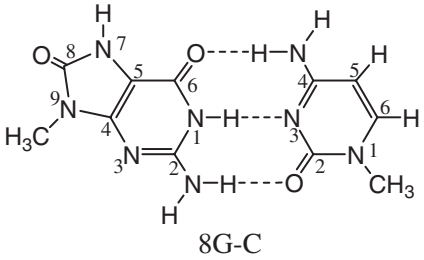

Figure 1. Schematic representation of hydrogen-bond base pair of 8-oxoguanine (8G) and cytosine (C).

Although the proton transfer in the $G^{\bullet+}$–C base pair was thoroughly examined experimentally and theoretically, the proton transfer in the $8G^{\bullet+}$–C base pair is not well characterized theoretically.

8G and $8G^{\bullet+}$ are generally repaired by several enzymes through the mechanism of base excision repair (BER). Recently, Milligan and co-workers have shown experimentally that the guanyl radical (G(-H)$^\bullet$) is restored to guanine by cresols and their substituted cresols.[38] It was concluded that the repair of radical proceeds through simultaneous one-step proton- and electron transfer. It is, then, expected that 8-oxoguanyl radical (8G(-H)$^\bullet$) is also repaired by phenol. Furthermore, experimental work has shown that G(-H)$^\bullet$ is repaired by 8G with the rate constant of 4.6×10^8 M^{-1} s^{-1} at pH 7.[39] However, there has been no theoretical work on proton transfer in G(-H)$^\bullet$–8G base pair and 8G(-H)$^\bullet$–phenol pair.

In this article, four reactions of hydrogen-bonding pairs are examined by quantum-chemical calculations.

R1: $8G^{\bullet+}$–C $\rightarrow$ 8G(-H)$^\bullet$–C(+H$^+$)$^+$ (1)

R2: PhOH–G(-H)$^\bullet$ $\rightarrow$ PhO$^\bullet$–G (2)

Published on the web February 4, 2011; doi:10.1246/bcsj.20100211

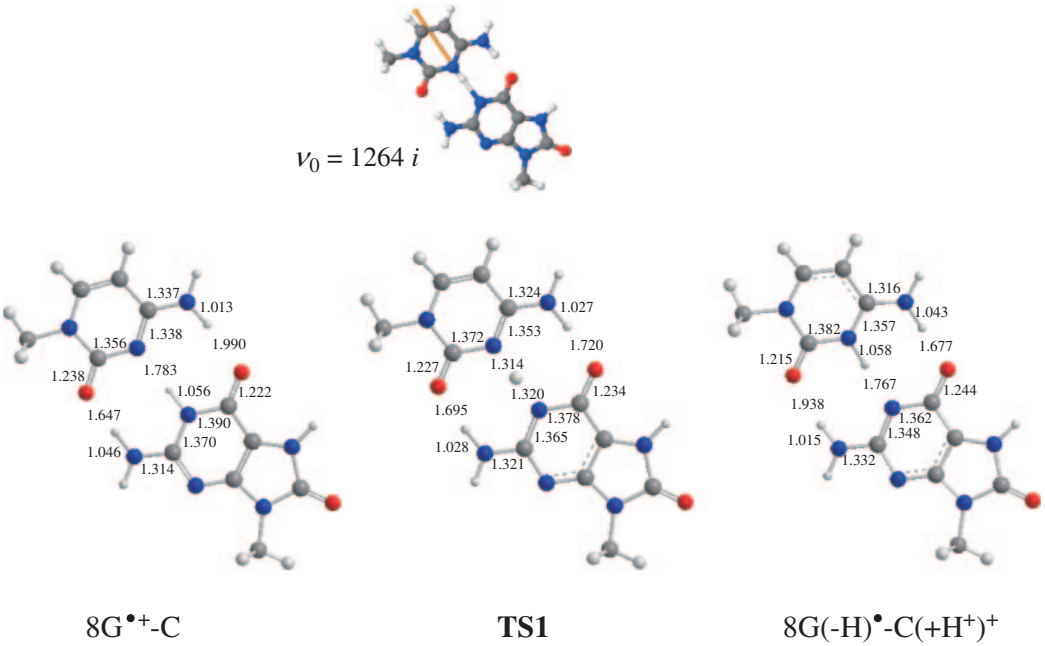

$8G^{\bullet+}$-C **TS1** $8G(-H)^{\bullet}$-$C(+H^{+})^{+}$

Figure 2. Optimized geometries for proton transfer of $8G^{\bullet+}$–C base pair. Imaginary frequency (cm^{-1}) and transition vector (orange arrow) of **TS1**. Distances are given in unit of Å. Transition vector is drawn by using a free soft Jmol.

R3: $PhOH–8G(-H)^{\bullet} \rightarrow PhO^{\bullet}–8G$ (3)

R4: $8G–G(-H)^{\bullet} \rightarrow 8G(-H)^{\bullet}–G$ (4)

The reaction **R1** presents the proton transfer to yield 8-oxoguanyl radical from radical cation of 8-oxoguanine. The reactions **R2**, **R3**, and **R4** show repair of guanyl or 8-oxogunyl radical to neutral base through proton- and electron transfer.

Computational Details

As shown in Figure 1, the N9 sites of 8G and N1 site of C are substituted by a methyl group instead of sugar. The hybrid exchange-correlation density functional method B3LYP[40,41] and the basis set 6-311G(2d,2p)[42,43] were employed. The geometric parameters of reactants, products, and transition states of reactions of **R1**–**R4** were fully optimized without any constraints. Theoretical calculations were performed adiabatically for the gas phase. For the stationary geometries, we performed frequency analyses to confirm the local minimum or transition state on the potential energy surface. The enthalpy and Gibbs free energies were estimated at room temperature of 298.15 K. Basis set superposition error (BSSE) correction was not taken into account for estimations of all relative energies. The program package Gaussian03 was used for all calculations.[44]

Results and Discussion

Proton Transfer in $8G^{\bullet+}$–C Radical Cation Base Pair (R1). As shown in Table 1, the vertical and adiabatic ionization potentials (IPs) of 8G are, respectively, 7.37 and 7.03 eV lower than 7.69 and 7.32 eV of G. These decreases of IPs show that 8G is more easily one-electron oxidized than G. The 8G–C base pair has lower IPs, 6.69 and 6.34 eV, vertically and adiabatically, respectively. These indicate that the 8G–C base pair is most easily ionized. The one-electron-oxidized 8G–C base pair has Mulliken charge populations of 0.776 and 0.224 e for the 8G and C moieties, respectively, while spin population is entirely localized on the 8G moiety with the value of 1.0 e. Thus, the one-electron-oxidized 8G–C base pair is formally presented as an $8G^{\bullet+}$–C radical cation base pair.

Table 1. Ionization Potentials (eV) of 8-Oxoguanine (8G) and Guanine (G) and Their Pairs with Cytosine Estimated at B3LYP/6-311G(2d,2p) Level

	Vertical IP	Adiabatic IP
8G	7.37	7.03
8G–C	6.69	6.34
G	7.69	7.32
G–C	6.94	6.54

Figure 2 shows the optimized geometries of the $8G^{\bullet+}$–C base pair, transition state (**TS1**) of the proton transfer, and the product. For the product, 8G moiety has charge and spin populations of 0.223 and 1.002 e, respectively, while C moiety has 0.777 and −0.002 e. It is apparent that 8G is presented as $8G(-H)^{\bullet}$ and C as $C(+H^{+})^{+}$. It is therefore found that the reaction **R1** proceeds to produce the $8G(-H)^{\bullet}$–$C(+H^{+})^{+}$ base pair under the single proton transfer from N1($8G^{\bullet+}$) to N3(C), which is similar to the single proton transfer in the $G^{\bullet+}$–C base pair.[23]

As found from Table 2, the binding free energy between $8G^{\bullet+}$ and C bases is 29.7 kcal mol^{-1} (ΔG) larger than 14.9 kcal mol^{-1} of 8G and C,[45] showing that the hydrogen bonds in the $8G^{\bullet+}$–C base pair are enhanced from the neutral 8G–C base pair. The binding free energy of $8G(-H)^{\bullet}$ and $C(+H^{+})^{+}$ bases was estimated to be 27.2 kcal mol^{-1} (ΔG) which is almost the same as the binding energy of 29.7 kcal mol^{-1} in the $8G^{\bullet+}$–C base pair, indicating that the strength of the hydrogen bonds is similar for both base pairs. Only ΔG is significantly small, compared with ΔE, ΔE_{ZPC}, and ΔH. This is due to decrease of entropy by binding two nucleobases.

Table 2. Binding Energies (kcal mol^{-1}) of Base Pairs[a)]

A–B	ΔE	ΔE_{ZPC}	ΔH	ΔG
8G$^{\bullet+}$–C	43.7	42.2	42.3	29.7
8G(-H)$^{\bullet}$–C(+H^{+})$^{+}$	42.1	40.5	40.8	27.2
PhOH–G(-H)$^{\bullet}$	14.3	12.8	12.6	2.0
PhO$^{\bullet}$–G	13.5	12.4	11.8	2.0
PhOH–8G(-H)$^{\bullet}$	13.7	12.1	12.0	0.8
PhO$^{\bullet}$–8G	13.8	12.9	12.3	2.4
8G–G(-H)$^{\bullet}$	29.0	27.9	27.9	15.6
8G(-H)$^{\bullet}$–G	26.8	25.3	25.4	12.5

a) Binding energy of A–B is estimated by ΔE(A–B) = E(A) + E(B) − E(A–B).

For the 8G$^{\bullet+}$–C base pair, the hydrogen-bond distances of N3(C)–H and O2(C)–H are given by 1.783 and 1.647 Å (Figure 2), respectively, while the bond distances of N1(8G)–H, N2(8G)–H, and N4(C)–H are 1.056, 1.046, and 1.013 Å. The frequencies corresponding to the stretching mode of N1(8G)–H, N2(8G)–H, and N4(C)–H were respectively estimated to be 2759, 2930, and 3481 cm^{-1}, in harmony with ordering of the bond distances. For the **TS1**, a single imaginary frequency of 1264i cm^{-1} was obtained. The transition vector shows that the proton transfers from N1(8G) to N3(C) and the proton is located at midpoint between N1(8G) and N3(C) at **TS1**. The bond distances of N2(8G)–H and N4(C)–H shorten and lengthen from 1.046 to 1.028 Å and from 1.013 to 1.027 Å, respectively. For the 8G(-H)$^{\bullet}$–C(+H^{+})$^{+}$ base pair, the strong hydrogen bonds shifted from N3(C)–H and O2(C)–H in the 8G$^{\bullet+}$–C base pair to N1(8G)–H and O6(8G)–H. Actually, the N1(8G)–H and O6(8G)–H distances are 1.767 and 1.677 Å, while N3(C)–H and O2(C)–H distances are 1.783 and 1.647 Å. The bond distances of N2(8G)–H, N3(C)–H, and N4(C)–H are, respectively, 1.015, 1.058, and 1.043 Å. This order of bond lengths reflects the order of the corresponding frequencies of 3457, 2714, and 2973 cm^{-1}. The frequencies of the N2(8G)–H and N4(C)–H bonds have blue- and red-shifted from 2930 to 3457 and from 3481 to 2973 cm^{-1}, respectively, with changes from the reactant to product.

Figure 3 shows the free energy diagram of the proton transfer. The activation energy of the proton transfer is 2.2 kcal mol^{-1} ($\Delta G^{\dagger}$), remarkably smaller than 11.4 kcal mol^{-1} [45] of the double proton transfer in the 8G–C base pair and comparable with 2.6 kcal mol^{-1} [45] of the G$^{\bullet+}$–C base pair. As found in Table 3, the $\Delta G^{\dagger}$-value is nearly equal to the $\Delta H^{\dagger}$ and $\Delta E_{ZPC}{}^{\dagger}$ values, while it is less than 4.5 kcal mol^{-1} of $\Delta E^{\dagger}$, indicating that the thermal contribution is important to evaluate the activation energy in the gas phase. The reaction of the proton transfer is endothermic by 0.7 kcal mol^{-1} (ΔG), which is also remarkably smaller than 9.1 kcal mol^{-1} [45] of the 8G–C base pair and is slightly less than 1.1 kcal mol^{-1} [45] of the G$^{\bullet+}$–C base pair. The ratio of the 8G$^{\bullet+}$–C and 8G(-H)$^{\bullet}$–C(+H^{+})$^{+}$ base pairs is 76.5 and 23.5% at the equilibrium state. Accordingly, this proton-transfer process is kinetically favored with small activation energy, while it is not favored thermodynamically.

Repair of G(-H)$^{\bullet}$ Neutral Radical by Phenol (R2). Figure 4a shows optimized geometry of a pair of guanyl radical (G(-H)$^{\bullet}$) and phenol (PhOH). An H-atom (OH in PhOH) makes a hydrogen bond to lone pair electrons at the N1 site of G(-H)$^{\bullet}$ with bond distance of 1.835 Å. H-atom (NH$_2$ in G(-H)$^{\bullet}$) also makes a hydrogen bond to lone pair electrons on O(PhOH) with bond distance of 2.109 Å. No hydrogen bond is formed between lone pair electrons on O6(G(-H)$^{\bullet}$) and H(PhOH) due to the long distance of 2.852 Å. Figure 5 shows the side view of the pair. Two molecular planes of G(-H)$^{\bullet}$ and PhOH are not coplanar with an angle of 38.6°. This may be due to steric hindrance which comes from two hydrogen bonds. The binding free energies of the PhOH–G(-H)$^{\bullet}$ pair (in Table 2) are given as ΔG = 2.0 kcal mol^{-1}. Table 4 summarizes Mulliken charge and spin densities for the reaction in the PhOH–G(-H)$^{\bullet}$ pair. The spin density is completely localized on G, indicating that G is a guanyl radical (G(-H)$^{\bullet}$) and small charge delocalization is induced from G(-H)$^{\bullet}$ to PhOH. Apparently, the reactant is the PhOH–G(-H)$^{\bullet}$ pair.

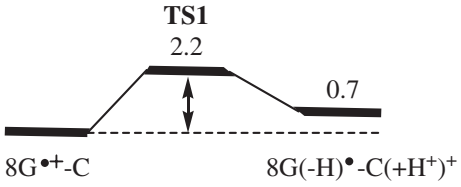

Figure 3. Free energy diagram of proton transfer in the 8G$^{\bullet+}$–C base pair. Energy values are given in unit of kcal mol^{-1}.

Table 3. Energetics (kcal mol^{-1}) for Proton Transfer of 8G$^{\bullet+}$–C, PhOH–G(-H)$^{\bullet}$, PhOH–8G(-H)$^{\bullet}$, and 8G–G(-H)$^{\bullet}$ Pairs

	$\Delta E^{\dagger}$	ΔE	$\Delta E_{ZPC}{}^{\dagger}$	ΔE_{ZPC}	$\Delta H^{\dagger}$	ΔH	$\Delta G^{\dagger}$	ΔG
8G$^{\bullet+}$–C	4.5	0.4	2.1	0.7	1.8	0.6	2.2	0.7
PhOH–G(-H)$^{\bullet}$	6.1	−7.1	2.7	−7.0	2.6	−6.9	2.9	−7.1
PhOH–8G(-H)$^{\bullet}$	9.5	1.4	6.0	0.8	5.8	1.1	6.6	0.6
8G–G(-H)$^{\bullet}$	5.9	−7.2	3.0	−6.3	2.6	−6.4	2.9	−6.2

After the proton transfer completed, two hydrogen bonds are formed between H(N1(G)) and O(PhO) with a distance of 1.904 Å and between O6(G) and H(PhO) with distance of 2.270 Å. Accordingly, two hydrogen bonds shifts from N1 and N2 of G(-H)$^{\bullet}$ to N1 and O6 of G. Two molecular planes become coplanar with a remarkable decrease in angle from 38.6 to 10.5°. The spin density is completely localized on PhO, indicating that PhO is formally a neutral pheoxyl radical PhO$^{\bullet}$. Accordingly, the product is presented as a PhO$^{\bullet}$–G pair. Although the radical transfers from G to PhOH moieties, it is expected that one electron in PhOH transfers to G(-H)$^{\bullet}$ with the proton transfer. From Table 3, the product, PhO$^{\bullet}$–G pair, is 7.1 kcal mol^{-1} more stable than the PhOH–G(-H)$^{\bullet}$ pair. These results show that the proton transfer in the PhOH–G(-H)$^{\bullet}$ pair easily proceeds to yield the PhO$^{\bullet}$–G pair.

It is found from Figure 6 that the transition state has a single imaginary frequency of 1575i cm^{-1}. Apparently the transition vector shows that **TS2** is the transition state of the proton transfer in PhOH–G(-H)$^{\bullet}$ pair with movement of H-atom at OH of PhOH toward N1(G(-H)$^{\bullet}$). The proton is shifted by 0.197 Å from the PhOH, indicating that the transition state is located at the early stages of reaction. It is found from Table 5 that the interatomic distances of N1(G(-H)$^{\bullet}$)–O and O6(G(-H)$^{\bullet}$)–C remarkably shorten from 2.754 to 2.462 Å and from 3.894 to

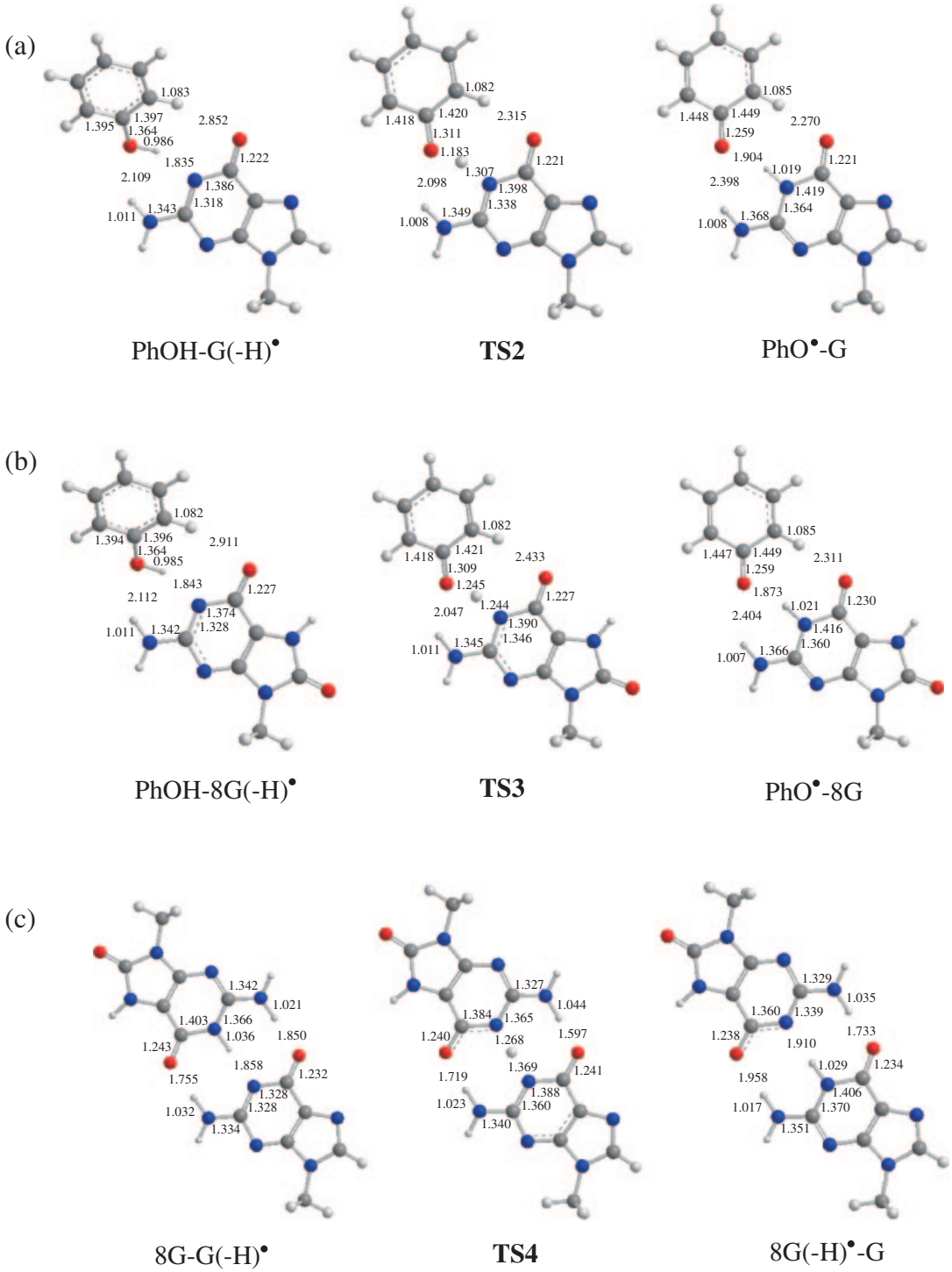

Figure 4. Optimized geometries for proton transfer of PhOH–G(-H)•, PhOH–8G(-H)•, and 8G–G(-H)• base pairs. Distances are given in unit of Å.

3.364 Å, respectively. This indicates that a weak hydrogen bond between O6(G(-H)•) and H(PhOH) is formed at 2.315 Å at **TS2**. On the pathway of the proton transfer, the angle of two molecular planes decreases from 38.6° of the PhOH–G(-H)• pair to 8.9° of **TS2**, making two molecular planes coplanar. Figure 7a shows the free energy diagram of the proton transfer. The activation energy was estimated to be 2.9 kcal mol^{-1} (ΔG), which is slightly higher than 1.26 and 1.72 kcal mol^{-1} estimated at the B3LYP/6-31G** and B3LYP/6-311++G** levels, respectively.[46] From Table 3, $\Delta G^{\dagger} = 2.9$, $\Delta H^{\dagger} = 2.6$, and $\Delta E_{ZPC}{}^{\dagger} = 2.7$ kcal mol^{-1}, while $\Delta E^{\dagger} = 6.1$ kcal mol^{-1}. $\Delta G^{\dagger}$ is decreased by 3.2 kcal mol^{-1} from $\Delta E^{\dagger}$, indicating that the thermal corrections are essential. The transferring H possesses positive charge density of 0.232 e and no spin density of −0.003 e. The corresponding PhO has negative charge of −0.246 e. The transferring H is obviously a proton. Figure 8

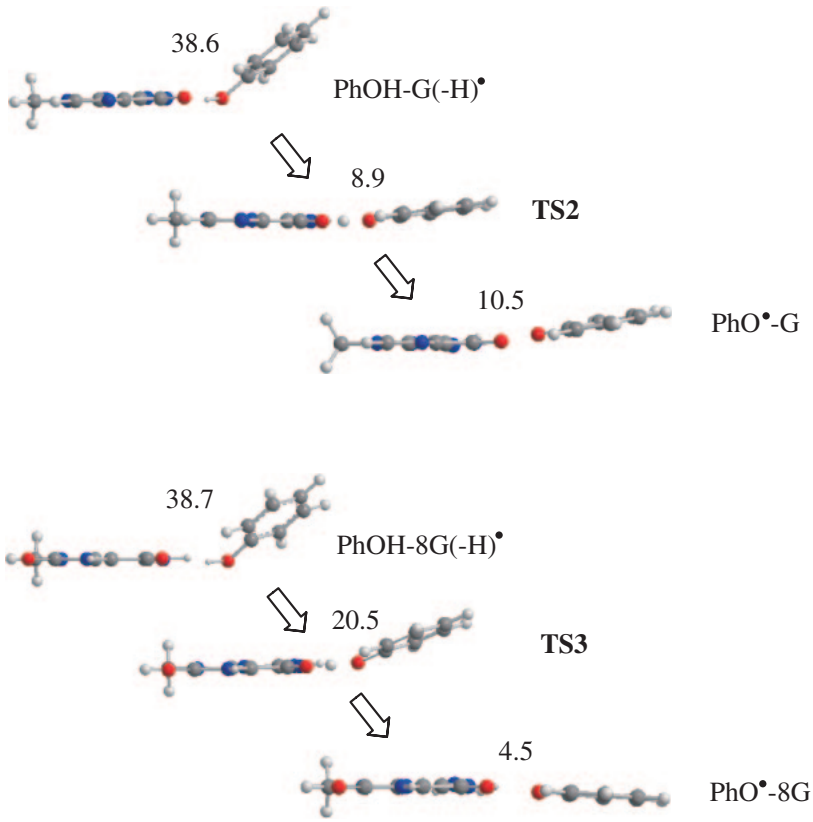

Figure 5. Side views of reactant, transition state, and product of proton transfer in guanyl radical–phenol and 8-oxoguanyl radical–phenol complexes. Numerical values are angles of two molecular planes given in degree.

Table 4. Mulliken Charge and Spin Densities for Reactions in PhOH–G(-H)•, 8G–PhO•, and 8G–G(-H)• Pairs

Complexes		Charge density			Spin density		
		Reactant	TS	Product	Reactant	TS	Product
PhOH–G(-H)•	G	0.073	0.013	−0.184	1.000	0.613	0.001
	PhOH	−0.073	−0.246	0.184	0.000	0.392	0.999
	H[a)]		0.232			−0.003	
8G–PhO•	PhOH	0.028	−0.306	−0.070	0.993	0.355	0.000
	8G	−0.028	0.083	0.070	0.007	0.646	1.000
	H[a)]		0.223			−0.001	
8G–G(-H)•	G	0.002	−0.154	−0.058	0.903	0.394	0.003
	8G	−0.002	0.044	0.058	0.097	0.605	0.997
	H[a)]		0.110			0.000	

a) Transferring H.

shows change of radical orbital through the proton transfer. The radical orbital of G(-H)• is apparently a π-orbital. At **TS2**, this radical orbital strongly interacts with a doubly occupied π orbital of PhOH since two molecular planes are coplanar. The π-radical orbital is combined in antibonding manner, consistent with a two-orbital and three-electron system. In the PhO•–G pair, the radical orbital is the π-orbital of PhO•. These changes show that one electron in the doubly occupied π orbital of PhOH transfers to occupy the radical π orbital of G(-H)•. Accordingly, in this reaction, one proton and one electron simultaneously transfer from the same donor (PhOH) to the same acceptor (G(-H)•), that is, this reaction proceeds in a proton-coupled electron-transfer (PCET) manner. The proton transfers through a σ-path, while electron transfers through a π-path. This conclusion is in good agreement with the experimental proposal.[38]

From Figure 7, the reaction for PhOH + G(-H)• → PhO• + G is 7.2 kcal mol^{-1} exothermic with the activation energy of 0.9 kcal mol^{-1}. It was observed by Milligan and coworkers that $\Delta G = 41$ kJ mol^{-1} (9.8 kcal mol^{-1}) is the driving force for overall reaction of *p*-cresol and guanyl radical.[38] This discrepancy for ΔG would be due to different conditions of estimations: plasmid DNA and the gas phase. However, when G(-H)• and PhOH encounter in the gas phase, G(-H)• is easily converted to G to make the repaired G–C pair.

Repair of 8G(-H)• Neutral Radical by Phenol (R3). As shown in Figure 4b, 8G(-H)• can make a pair with PhOH. It is confirmed that the reactant is really a PhOH–8G(-H)• pair from

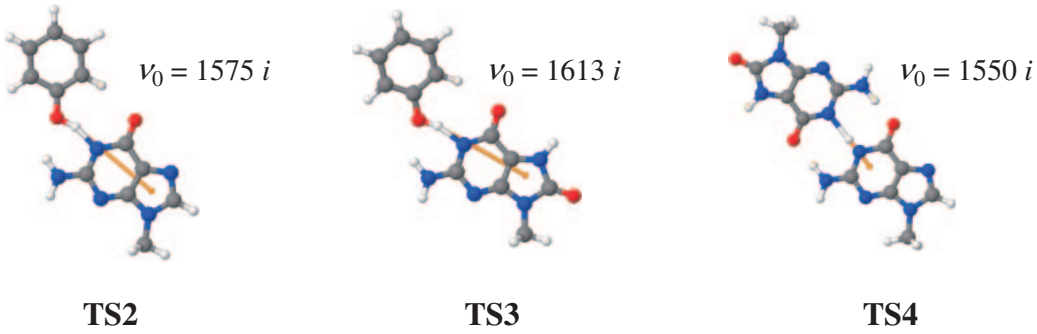

Figure 6. Imaginary frequencies (cm^{-1}) and transition vectors (orange arrow) corresponding to **TS2**, **TS3**, and **TS4**. Transition vectors are drawn by using a free soft Jmol.

Table 5. Selected Distances (Å) between Heavy Atoms Corresponding to Hydrogen Bonds

A–B	N1(G)–O	O6(G)–C	N2(G)–O	N1(G)–N1(8G)	O6(G)–N2(8G)	N2(G)–O6(8G)
PhOH–G(-H)$^\bullet$	2.754	3.894	2.956			
TS2	2.462	3.364	2.868			
PhO$^\bullet$–G	2.893	3.345	3.230			
PhOH–8G(-H)$^\bullet$	2.761	3.953	2.964			
TS3	2.459	3.475	2.835			
PhO$^\bullet$–8G	2.866	3.386	3.224			
8G–G(-H)$^\bullet$				2.893	2.871	2.787
TS4				2.637	2.640	2.740
8G(-H)$^\bullet$–G				2.937	2.769	2.974

the spin population shown in Table 4. The pattern of the hydrogen bonds is the same as that of PhOH–G(-H)$^\bullet$ pair. Actually, from Table 5 and Figure 5, the interatomic distances corresponding to the hydrogen bond and the angle of the molecular planes are the same. Furthermore, from Figure 7, the binding energy (ΔG) of the PhOH–8G(-H)$^\bullet$ pair is 0.8 kcal mol^{-1}, slightly smaller than 2.0 kcal mol^{-1} for the PhOH–G(-H)$^\bullet$ pair. These show that the characteristics of the PhOH–8G(-H)$^\bullet$ pair are exactly the same as those of the PhOH–G(-H)$^\bullet$ pair.

It also seems from Figure 4b that the optimized geometry of the product after completion of the proton transfer is similar to that of the PhO$^\bullet$–G pair. The spin density is completely localized on PhO, indicating that PhO is formally a neutral phenoxyl radical PhO$^\bullet$. Accordingly, the product is designated as a PhO$^\bullet$–8G pair. Although the radical transfers from 8G to PhOH moieties, it is expected that one electron in PhOH transfers to 8G(-H)$^\bullet$ with the proton transfer. However, the angle of two molecular planes was estimated to be 4.5°, in contrast with 10.5° of the PhO$^\bullet$–G pair. A remarkable difference from the PhO$^\bullet$–G pair is found in heat of reaction for the proton transfer. Although the proton transfer in the PhOH–G(-H)$^\bullet$ pair is 7.1 kcal mol^{-1} exothermic, the proton transfer in the PhOH–8G(-H)$^\bullet$ pair is 0.6 kcal mol^{-1} endothermic. The ratio of the PhOH–8G(-H)$^\bullet$ and PhO$^\bullet$–8G pairs is estimated to be 71.7 and 28.3%, respectively at the equilibrium state. Accordingly, it is hard to induce the proton transfer from PhOH–8G(-H)$^\bullet$ pair thermodynamically.

It is obvious from Figure 6 that **TS3** is the transition state that the proton transfers from PhOH to N1(8G(-H)$^\bullet$) with single imaginary frequency of 1613i cm^{-1}. The transferring proton is located at the middle point between PhOH and N1, in contrast to 0.197 Å shifted from PhOH in **TS2**. It is, then, expected that **TS3** is at a middle stage of the proton transfer between reactant and product and not at an early stage like **TS2**. The angle of two molecular planes was estimated to be 20.5° (Figure 5) which is significantly larger than 8.9° of **TS2**. From Figure 7b, the activation energy from the PhOH–8G(-H)$^\bullet$ pair was estimated to be 6.6 kcal mol^{-1} which is 3.7 kcal mol^{-1} higher than **TS2**. Thus, the proton transfer in the PhOH–8G(-H)$^\bullet$ pair will be kinetically less favorable, in contrast with the PhOH–G(-H)$^\bullet$ pair. Conversely, the backward reaction; PhO$^\bullet$–8G → PhOH–8G(-H)$^\bullet$ is favored thermodynamically and kinetically.

It can be seen from Table 3 that the energy differences (ΔE) of the 8G$^{+\bullet}$–C and PhOH–8G(-H)$^\bullet$ pairs are small values of 0.4 and 1.4 kcal mol^{-1}, respectively. We carried out calculations to confirm that the BSSE correction does not affect the energy differences. Table 6 summarizes the binding energies of pairs (ΔE_b), relative energies between pairs (ΔE_{rel}), and activation energies of proton transfer ($\Delta E^\dagger$). Although ΔE_bs are decreased by 2.9–3.4 kcal mol^{-1}, each pair is stable with strong hydrogen bonds. The differences of the ΔE_{rel} values between with and without BSSE corrections are remarkably small and the differences of $\Delta E^\dagger$ values are also small. These trials show that the BSSE correction is sufficiently small. It will be expected that the BSSE correction for ΔG is small, since the optimized geometries with and without BSSE corrections are almost the same.

Since it has been made clear that the backward reaction of **R3** is favored, hereafter, we would like to change our discussion for new reaction **R3** where the reactant and product are exchanged in the original **R3**, as follows,

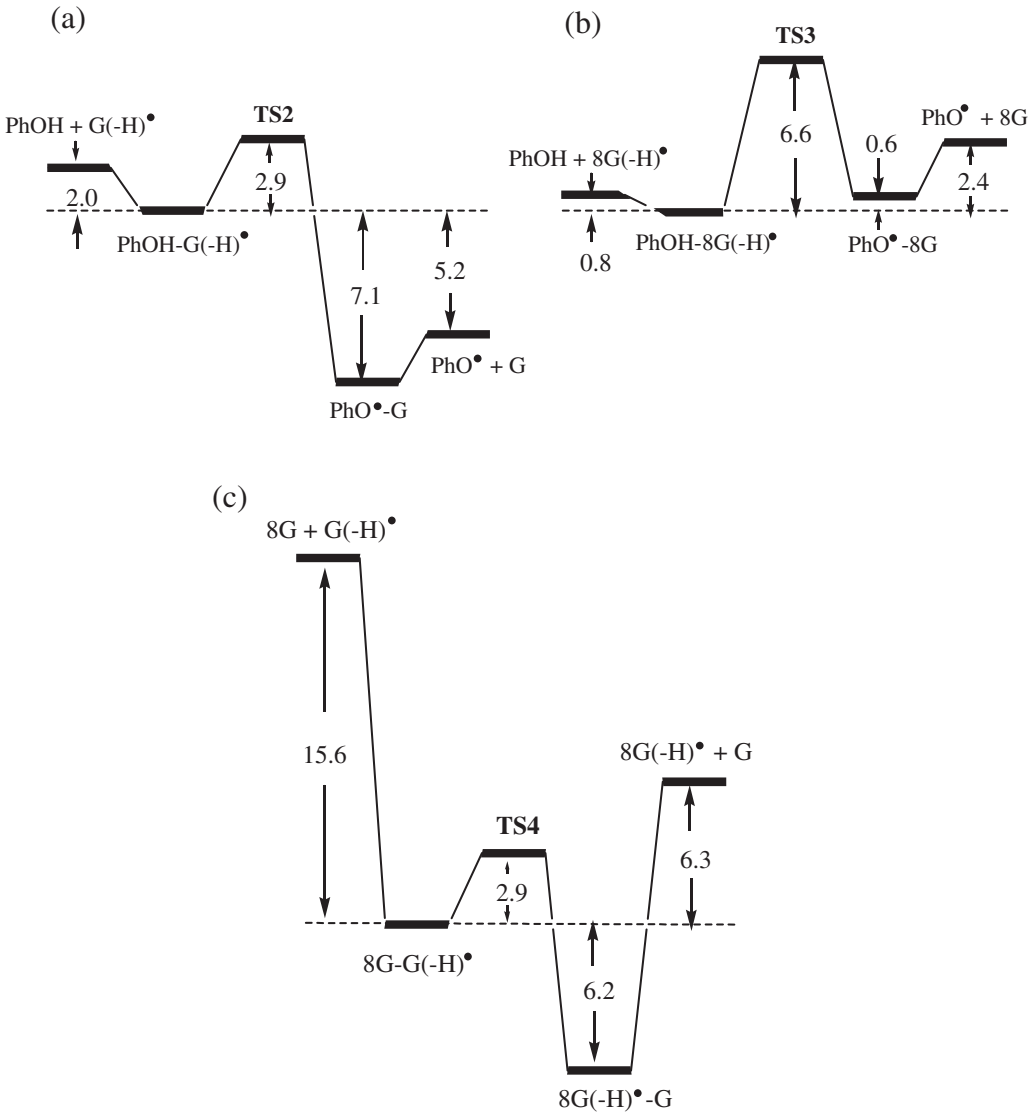

Figure 7. Free energy diagrams of proton transfer of PhOH–G(-H)• pair (a), PhOH–8G(-H)• pair (b), and 8G–G(-H)• base pair (c). Energy values are given in unit of kcal mol^{-1}.

R3: PhO•–8G → PhOH–8G(-H)• (5)

From Table 4, the Mulliken charge density of the transferring H is a positive value of 0.223 e and the spin density is zero at **TS3**, indicating that the transferring H is a proton. The spin densities of 8G and PhOH are 0.646 and 0.355 e, respectively. It is found from Figure 8 that the radical orbital distribute over both 8G and PhO. This indicates that one electron in doubly occupied π-orbital of 8G transfers to the radical π-orbital of PhO• at the same time of the proton transfer. The proton transfers through a σ-path, while an electron transfers through a π-path under the PCET mechanism, which are the same as those of the PhOH–G(-H)• pair.

For the overall reaction of PhO• + 8G → PhOH + 8G(-H)•, the forward reaction proceeds in an exothermic manner with 1.6 kcal mol^{-1} and has the activation energy of 4.2 kcal mol^{-1}. Namely, the encounter of 8G and PhO• induces the proton- and electron transfer from 8G to PhO• to yield PhOH + 8G(-H)•. This is in good agreement with the experimental proposal by Steenken and co-workers.[39] Rate constants for the overall reaction were estimated to be 8.3×10^8 and 5.6×10^7 s^{-1} for the forward and backward reactions, respectively. In aqueous solution, those are estimated to be 2.6×10^9 and 2.6×10^7 M^{-1} s^{-1} experimentally.[39] The discrepancy is due to different conditions of the gas phase and aqueous solution. Direct comparison must be made under the conditions of the PCM correction or cluster with water molecules. We would like to leave this problem as a future investigation.

Repair of G(-H)• Neutral Radical by 8G (R4). Figure 4c shows the optimized geometries of the 8G–G(-H)• base pair, the transition state (**TS4**) of proton transfer, and the 8G(-H)•–G base pair. It can be confirmed that the radical configuration of the reactant and product are, respectively, 8G–G(-H)• and 8G(-H)•–G base pairs from the spin population shown in Table 4. It is also confirmed from Figure 6 that **TS4** is the transition state of the proton transfer from 8G to G(-H)• with a single imaginary frequency of 1550i cm^{-1}. The 8G–G(-H)• base pair has a perfectly coplanar geometry and has three hydrogen

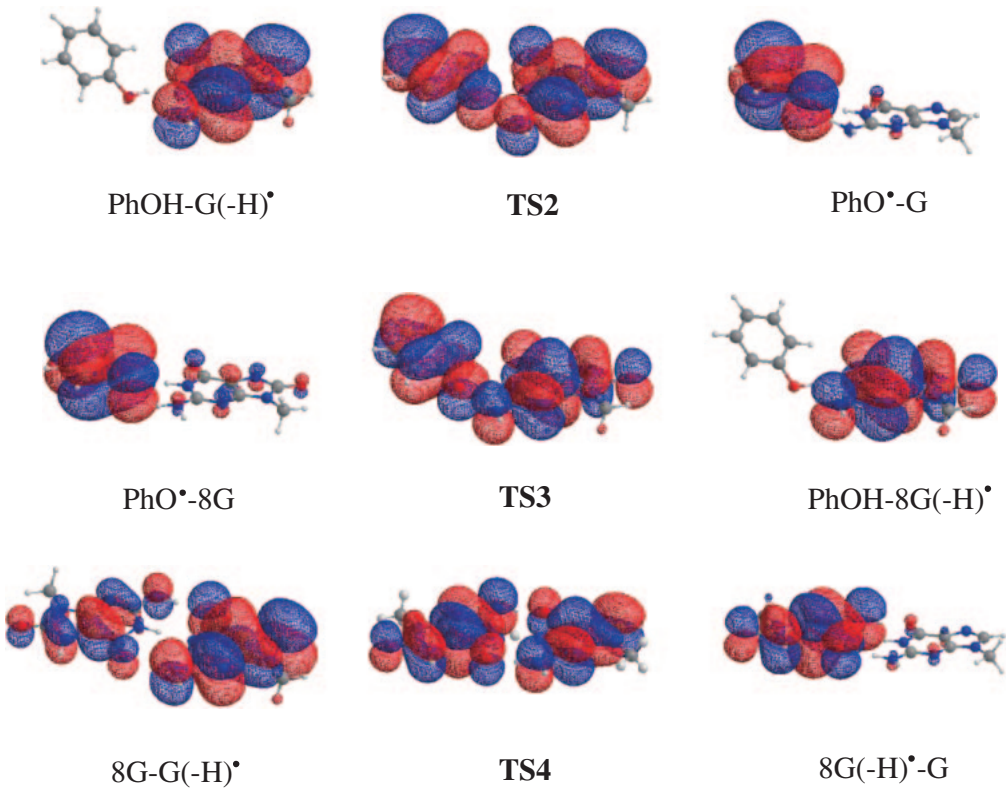

Figure 8. Changes of radical orbital for proton transfer in PhOH–G(-H)•, PhO•–8G, and 8G–G(-H)• pairs.

Table 6. Energetic Corrected by BSSE for Base Pairs in Unit of kcal mol^{-1}

Complexes	ΔE_b[a)]	ΔE_{rel}[b)]	$\Delta E^{\dagger}$[c)]
8G$^{\bullet+}$–C	40.3 (43.7)[d)]	0.0	5.0 (4.5)
8G(-H)•–C(+H$^+$)$^+$	38.7 (42.1)	0.4 (0.4)	
PhOH–8G(-H)•	10.4 (13.7)	0.0	9.9 (9.5)
PhO•–8G	10.9 (13.8)	1.2 (1.4)	

a) Binding energies of base pairs. b) Heat of reaction for proton transfer. c) Geometries optimized without BSSE correction are employed. d) Numerical values in parentheses are ones estimated without BSSE correction, which are also shown in Tables 2 and 3.

bonds of O6(8G)–H, H–N1(G(-H)•), and H–O6(G(-H)•). The binding free energy (ΔG) was estimated to be 15.6 kcal mol^{-1}, as shown in Table 2 and Figure 7c. The pattern of three hydrogen bonds can be compared with those of the 8G–C base pair (Figure 1), since both base pairs are neutral, and N3(C) and N1(G(-H)•) have common lone pair electrons in the molecular plane. The hydrogen-bond distances of O6(8G)–H, H–N1 (G(-H)•), and H–O6(G(-H)•) in the 8G–G(-H)• base pair are 1.755, 1.858, and 1.850 Å, respectively, in fairly good agreement with 1.771, 1.896, and 1.914 Å in the 8G–C base pair.[45] The binding energy of $\Delta G = 15.6$ and $\Delta E = 29.0$ kcal mol^{-1} of the 8G–G(-H)• base pair are also in good agreement with $\Delta G = 14.9$ and $\Delta E = 27.8$ kcal mol^{-1} of the 8G–C base pair.[45] These show that the hydrogen-bond interaction is due to σ-type interaction without influence of π-electrons of nucleobases.

The optimized geometry of the transition state (**TS4**) for the proton transfer from 8G to G(-H)• is coplanar as shown in Figure 4. From Table 5, the atomic distance of N1(G(-H)•)–N1(8G), which corresponds to the site of proton transfer, decreases by 0.256 Å from 2.893 Å of the reactant 8G–G(-H)• base pair, which is smaller than 0.292 Å from 2.754 Å of the PhOH–G(-H)• pair and 0.407 Å from 2.866 Å of the 8G–PhO• pair. The transferring H is shifted by 0.232 Å from 8G, showing that **TS4** is located at an early stage of the proton transfer. The activation free energy of proton transfer in the 8G–G(-H)• base pair was estimated to be 2.9 kcal mol^{-1}, in coincidental agreement with 2.9 kcal mol^{-1} in the PhOH–G(-H)• pair. Accordingly the proton transfer from 8G to G(-H)• is favored with a small energy barrier.

The optimized geometry of the produced 8G(-H)•–G base pair remains coplanar, as shown in Figure 4c. From Figure 7c, the 8G(-H)•–G base pair is 6.2 kcal mol^{-1} (ΔG) lower than the 8G–G(-H)• base pair, indicating that the proton transfer in the 8G–G(-H)• base pair is exothermic. Thus the free energy diagram from the 8G–G(-H)• to 8G(-H)•–G pairs is quite similar to that from the PhOH–G(-H)• to PhO•–G pairs, as can be seen from Figures 7a and 7c. Three hydrogen bonds of the 8G(-H)•–G base pair can be also compared with those of the G–C base pair (Figure 1). The hydrogen bond distances of O6(8G(-H)•)–H, N1(8G(-H)•)–H, and O6(G)–H in the 8G(-H)•–G base pair are, respectively, 1.958, 1.910, and 1.733 Å, in fairly good agreement with the corresponding distances of 1.918, 1.920, and 1.764 Å in the G–C base pair.[45] The binding energy of $\Delta G = 12.5$ and $\Delta E = 26.8$ kcal mol^{-1} (Table 2) of the 8G(-H)•–G base pair are also in good agreement with $\Delta G = 14.2$ and $\Delta E = 27.3$ kcal mol^{-1} of the G–C base pair. Similar to the 8G–G(-H)• base pair, the hydrogen-bond interaction is due to σ-type interaction without influence of π-electrons of nucleobases.

The free energy diagram for the overall reaction of 8G + G(-H)$^{\bullet}$ → 8G(-H)$^{\bullet}$ + G is shown in Figure 7c. This diagram is different from two other diagrams. The behavior of reaction (**R4**) is completely different from reaction (**R3**) and is also distinct from that of reaction (**R2**) even the diagram of proton transfer within pair is similar. Accordingly, when G(-H)$^{\bullet}$ and 8G encounter, the proton transfer from 8G to G(-H)$^{\bullet}$ immediately proceeds without energy barrier and with exothermic energy of 9.3 kcal mol^{-1}. Steenken and co-workers have shown that a driving force for oxidation of 8-OHdG by G(-H)$^{\bullet}$ in the aqueous solution is 13 kcal mol^{-1}.[39] The discrepancy for ΔG would be due to different conditions of estimations: plasmid DNA and the gas phase.

From Table 4, at **TS4**, the transferring H has positive charge density of 0.110 e and no spin density. It is clear that the transferring H is a proton. For the 8G–G(-H)$^{\bullet}$ base pair, the spin of G(-H)$^{\bullet}$ distributes over 8G with 0.903 e and 0.097 e of 8G. We can see the π small lobe on 8G as shown in Figure 8. This may be due to interaction of a high energy π-orbital of 8G with radical π-orbital of G(-H)$^{\bullet}$. At **TS4**, spin densities of G(-H)$^{\bullet}$ and 8G are 0.394 e and 0.605 e, indicating that the radical spin mostly transfers from G to 8G, and distributes over a π antibonding orbital of G and 8G. Finally, a radical completely transfers from G to 8G. It is obvious that this reaction also proceeds with simultaneous transfer of a proton and an electron.

On Proton- and Electron Transfer. These three repair reactions proceed under the same PCET mechanism. However, as can be found in Table 4, the behaviors of charge and spin densities at the transition state of the reaction in PhOH–G(-H)$^{\bullet}$ pair are different from those of two other reactions. The spin densities of G(-H)$^{\bullet}$ and PhOH are, respectively, given by 0.613 e and 0.392 e, while those values are reversed in the 8G–PhO$^{\bullet}$ and 8G–G(-H)$^{\bullet}$ pairs. The charge densities of G(-H)$^{\bullet}$ and PhOH are, respectively, given by positive value of 0.013 e and negative value of −0.246 e, while those signs are reversed in the 8G–PhO$^{\bullet}$ and 8G–G(-H)$^{\bullet}$ pairs. In general, the PCET reaction of X–Y$^{\bullet}$ pair is simply represented as follows,

$$X \underset{H^+}{\overset{e^-}{\rightleftarrows}} Y^{\bullet} \tag{6}$$

Here, X = PhOH and Y$^{\bullet}$ = G(-H)$^{\bullet}$ for **R2**, X = 8G and Y$^{\bullet}$ = PhO$^{\bullet}$ for **R3**, and X = 8G and Y$^{\bullet}$ = G(-H)$^{\bullet}$ for **R4**. From Table 4, we can evaluate degree of hole transfer (positive charge) which Y$^{\bullet}$ has received from X through the σ-path in the course of the proton transfer. Suppose that its degree is χ(Y) (>0). The degree of electron transfer from X to Y through the π-path is equal to σ(X) (>0) which corresponds to the spin densities of X. The charge density of Y, ρ(Y), can be represented by χ(Y) and σ(X).

$$\rho(Y) = \chi(Y) - \sigma(X) \tag{7}$$

then

$$\chi(Y) = \sigma(X) + \rho(Y) \tag{8}$$

σ(X) and χ (Y) for three reactions **R2**, **R3**, and **R4** are summarized in Table 7. At the transition states, χ(G(-H)$^{\bullet}$) = 0.405 e for **R2**, χ(PhO$^{\bullet}$) = 0.340 e for **R3**, and χ(G(-H)$^{\bullet}$) = 0.451 e for **R4**. These indicate that the degrees of the hole transfer are nearly equal for three reactions. The differences among three reactions are strongly dependent on the degree of the electron transfer from the closed neutral species. At the transition state, for the reaction **R2**, the degrees of hole- and electron transfer that the G(-H)$^{\bullet}$ moiety receives are the same. For the reactions **R3** and **R4**, the degrees of the electron transfer to the radical moiety are larger than the hole transfer. In other words, the rate of electron transfer is the same as that of proton transfer in the PhOH pair, while the rate of electron transfer is much larger than that of proton transfer in the 8G pairs. Accordingly, the 8G base can readily to release an electron.

Table 7. Degrees of Electron and Hole Transfer in PCET Reactions of X–Y$^{\bullet}$

Pair		Reactant	TS	Product
PhOH–G(-H)$^{\bullet}$	σ(PhOH)	0.000	0.392	0.999
	χ(G(-H)$^{\bullet}$)	0.073	0.405	0.815
8G–PhO$^{\bullet}$	σ(8G)	0.007	0.646	1.000
	χ(PhO$^{\bullet}$)	0.035	0.340	0.930
8G–G(-H)$^{\bullet}$	σ(8G)	0.097	0.605	0.997
	χ(G(-H)$^{\bullet}$)	0.099	0.451	0.939

Conclusion

The stability and proton transfer in the 8G$^{+\bullet}$–C base pair have been examined. The hydrogen bonds in the 8G$^{+\bullet}$–C base pair are enhanced much more than the 8G–C base pair. The dissociation energy of the 8G$^{+\bullet}$–C base pair is 29.7 kcal mol^{-1}, which is similar to 30.8 kcal mol^{-1} of G$^{+\bullet}$–C base pair. The single proton transfer in the 8G$^{+\bullet}$–C base pair proceeds from N1(8G$^{+\bullet}$) to N3(C) with the activation energy of 2.2 kcal mol^{-1}. The behavior of the proton transfer is the same as that of the G$^{+\bullet}$–C base pair. Accordingly, the oxo-atom at the C8 site of 8G does not influence the characteristics of the hydrogen bonds and proton transfer. It is believed that it is possible that the 8G$^{+\bullet}$–C base pair exists in DNA before the DNA polymerase misreads 8G as thymine.

The repairs of G(-H)$^{\bullet}$ and 8G(-H)$^{\bullet}$ bases to G and 8G have been studied by reaction with phenol, and the repair of G(-H)$^{\bullet}$ base has been also studied for the pair with the 8G base. These three reactions proceed by the PCET mechanism and the proton transfers through the σ-path, while the electron transfers through the π-path.

1) The PhOH–G(-H)$^{\bullet}$ pair is easily repaired to the PhO$^{\bullet}$–G pair with exothermic energy of 7.1 kcal mol^{-1}. The reaction of PhOH + G(-H)$^{\bullet}$ → PhO$^{\bullet}$ + G is 7.2 kcal mol^{-1} exothermic with the activation energy of 0.9 kcal mol^{-1}. Namely, when G(-H)$^{\bullet}$ and PhOH encounter, G(-H)$^{\bullet}$ is easily converted to G.

2) For the PhOH–8G(-H)$^{\bullet}$ pair, the reversed reaction, PhO$^{\bullet}$ + 8G → PhOH + 8G(-H)$^{\bullet}$, is favored. The reaction is 1.6 kcal mol^{-1} exothermic with the activation energy of 4.2 kcal mol^{-1}. This result is in fairly good agreement with the experimental results.

3) For 8G–G(-H)$^{\bullet}$ base pair, the PCET reaction proceeds with exothermic energy of 6.2 kcal mol^{-1} and the activation energy of 2.9 kcal mol^{-1}.

4) The 8G base is easily oxidized due to the high energy

HOMO and subsequently, $8G^{+\bullet}$ induces rapid deprotonation to yield $8G(-H)^{\bullet}$. When 8G encounters $PhO^{\bullet}$ or $G(-H)^{\bullet}$, the 8G easily delivers the proton and electron to yield PhOH or G. Accordingly, it is expected that 8G can protect the other bases and amino acids from oxidation.

This work was supported by the Grant-in-Aid for Scientific Research from the Ministry of Education, Culture, Sports, Science and Technology, Japan.

References

1 M. D. Sevilla, B. Besler, A.-O. Colson, *J. Phys. Chem.* **1995**, *99*, 1060.
2 C. A. M. Seidel, A. Schulz, M. H. M. Sauer, *J. Phys. Chem.* **1996**, *100*, 5541.
3 S. Steenken, S. V. Jovanovic, *J. Am. Chem. Soc.* **1997**, *119*, 617.
4 C. J. Burrows, J. G. Muller, *Chem. Rev.* **1998**, *98*, 1109.
5 I. Saito, M. Takayama, H. Sugiyama, K. Nakatani, A. Tsuchida, M. Yamamoto, *J. Am. Chem. Soc.* **1995**, *117*, 6406.
6 D. T. Breslin, G. B. Schuster, *J. Am. Chem. Soc.* **1996**, *118*, 2311.
7 H. Sugiyama, I. Saito, *J. Am. Chem. Soc.* **1996**, *118*, 7063.
8 E. D. A. Stemp, M. R. Arkin, J. K. Barton, *J. Am. Chem. Soc.* **1997**, *119*, 2921.
9 B. Armitage, D. Ly, T. Koch, H. Frydenlund, H. Ørum, H. G. Batz, G. B. Schuster, *Proc. Natl. Acad. Sci. U.S.A.* **1997**, *94*, 12320.
10 K. Nakatani, K. Fujisawa, C. Dohno, T. Nakamura, I. Saito, *Tetrahedron Lett.* **1998**, *39*, 5995.
11 I. Saito, T. Nakamura, K. Nakatani, Y. Yoshioka, K. Yamaguchi, H. Sugiyama, *J. Am. Chem. Soc.* **1998**, *120*, 12686.
12 Y. Yoshioka, Y. Kitagawa, Y. Takano, K. Yamaguchi, T. Nakamura, I. Saito, *J. Am. Chem. Soc.* **1999**, *121*, 8712.
13 L. P. Candeias, S. Steenken, *J. Am. Chem. Soc.* **1992**, *114*, 699.
14 T. Melvin, S. Botchway, A. W. Parker, P. J. O'Neill, *J. Chem. Soc., Chem. Commun.* **1995**, 653.
15 E. Meggers, D. Kusch, M. Spichty, U. Wille, B. Giese, *Angew. Chem., Int. Ed.* **1998**, *37*, 460.
16 S. Steenken, *Chem. Rev.* **1989**, *89*, 503.
17 L. P. Candeias, S. Steenken, *J. Am. Chem. Soc.* **1989**, *111*, 1094.
18 K. Kobayashi, S. Tagawa, *J. Am. Chem. Soc.* **2003**, *125*, 10213.
19 M. Hutter, T. Clark, *J. Am. Chem. Soc.* **1996**, *118*, 7574.
20 J. Bertran, A. Oliva, L. Rodríguez-Santiago, M. Sodupe, *J. Am. Chem. Soc.* **1998**, *120*, 8159.
21 X. Li, Z. Cai, M. D. Sevilla, *J. Phys. Chem. B* **2001**, *105*, 10115.
22 S. C. Weatherly, I. V. Yang, P. A. Armistead, H. H. Thorp, *J. Phys. Chem. B* **2003**, *107*, 372.
23 L. Sun, Y. Bu, *J. Phys. Chem. B* **2005**, *109*, 593.
24 L. Sun, Y. Y. Bu, *THEOCHEM* **2009**, *909*, 25.
25 A. Kumar, M. D. Sevilla, *J. Phys. Chem. B* **2009**, *113*, 11359.
26 A. Adhikary, D. Khanduri, M. D. Sevilla, *J. Am. Chem. Soc.* **2009**, *131*, 8614.
27 D. M. Close, *J. Phys. Chem. A* **2010**, *114*, 1860.
28 A. W. Parker, C. Y. Lin, M. W. George, M. Towrie, M. K. Kuimova, *J. Phys. Chem. B* **2010**, *114*, 3660.
29 M. Noguera, M. Sodupe, J. Bertrán, *Theor. Chem. Acc.* **2004**, *112*, 318.
30 C. Sheu, C. S. Foote, *J. Am. Chem. Soc.* **1995**, *117*, 474.
31 C. Sheu, C. S. Foote, *J. Am. Chem. Soc.* **1995**, *117*, 6439.
32 W. Adam, C. R. Saha-Möller, A. Schönberger, *J. Am. Chem. Soc.* **1997**, *119*, 719.
33 N. R. Jena, P. C. Mishra, *J. Phys. Chem. B* **2005**, *109*, 14205.
34 V. Verdolino, R. Cammi, B. H. Munk, H. B. Schlegel, *J. Phys. Chem. B* **2008**, *112*, 16860.
35 Y. Ye, J. G. Muller, W. Luo, C. L. Mayne, A. J. Shallop, R. A. Jones, C. J. Burrows, *J. Am. Chem. Soc.* **2003**, *125*, 13926.
36 B. H. Munk, C. J. Burrows, H. B. Schlegel, *J. Am. Chem. Soc.* **2008**, *130*, 5245.
37 F. Prat, K. N. Houk, C. S. Foote, *J. Am. Chem. Soc.* **1998**, *120*, 845.
38 J. R. Milligan, J. A. Aguilera, O. Hoang, A. Ly, N. Q. Tran, J. F. Ward, *J. Am. Chem. Soc.* **2004**, *126*, 1682.
39 S. Steenken, S. V. Jovanovic, M. Bietti, K. Bernhard, *J. Am. Chem. Soc.* **2000**, *122*, 2373.
40 A. D. Becke, *J. Chem. Phys.* **1993**, *98*, 1372.
41 C. Lee, W. Yang, R. G. Parr, *Phys. Rev. B* **1988**, *37*, 785.
42 A. D. McLean, G. S. Chandler, *J. Chem. Phys.* **1980**, *72*, 5639.
43 R. Krishnan, J. S. Binkley, R. Seeger, J. A. Pople, *J. Chem. Phys.* **1980**, *72*, 650.
44 M. J. Frisch, G. W. Trucks, H. B. Schlegel, G. E. Scuseria, M. A. Robb, J. R. Cheeseman, J. A. Montgomery, Jr., T. Vreven, K. N. Kudin, J. C. Burant, J. M. Millam, S. S. Iyengar, J. Tomasi, V. Barone, B. Mennucci, M. Cossi, G. Scalmani, N. Rega, G. A. Petersson, H. Nakatsuji, M. Hada, M. Ehara, K. Toyota, R. Fukuda, J. Hasegawa, M. Ishida, T. Nakajima, Y. Honda, O. Kitao, H. Nakai, M. Klene, X. Li, J. E. Knox, H. P. Hratchian, J. B. Cross, V. Bakken, C. Adamo, J. Jaramillo, R. Gomperts, R. E. Stratmann, O. Yazyev, A. J. Austin, R. Cammi, C. Pomelli, J. W. Ochterski, P. Y. Ayala, K. Morokuma, G. A. Voth, P. Salvador, J. J. Dannenberg, V. G. Zakrzewski, S. Dapprich, A. D. Daniels, M. C. Strain, O. Farkas, D. K. Malick, A. D. Rabuck, K. Raghavachari, J. B. Foresman, J. V. Ortiz, Q. Cui, A. G. Baboul, S. Clifford, J. Cioslowski, B. B. Stefanov, G. Liu, A. Liashenko, P. Piskorz, I. Komaromi, R. L. Martin, D. J. Fox, T. Keith, M. A. Al-Laham, C. Y. Peng, A. Nanayakkara, M. Challacombe, P. M. W. Gill, B. Johnson, W. Chen, M. W. Wong, C. Gonzalez, J. A. Pople, *Gaussian 03, Revision B.05*, Gaussian, Inc., Wallingford CT, **2004**.
45 Our calculations performed at B3LYP/6-311G(2d,2p) level.
46 N. R. Jena, P. C. Mishra, S. Suhai, *J. Phys. Chem. B* **2009**, *113*, 5633.